

Affordance-Aware Object Insertion via Mask-Aware Dual Diffusion

Jixuan He^{1,2,*} Wanhua Li^{1,*} Ye Liu^{1,3} Junsik Kim¹ Donglai Wei⁴ Hanspeter Pfister¹
¹Harvard University ²Cornell Tech ³The Hong Kong Polytechnic University ⁴Boston College

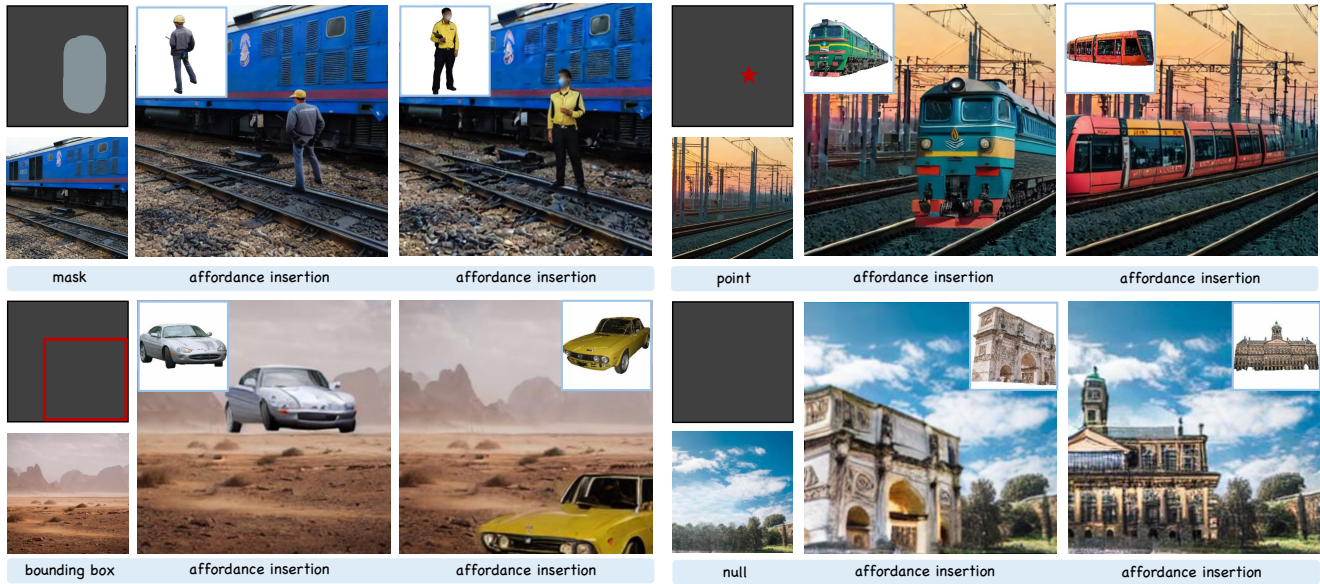


Figure 1. Given a foreground-background object-scene pair, our model can perform affordance-aware object insertion conditioning on different position prompts, including points, bounding boxes, masks, and even null prompts.

Abstract

As a common image editing operation, image composition involves integrating foreground objects into background scenes. In this paper, we expand the application of the concept of Affordance from human-centered image composition tasks to a more general object-scene composition framework, addressing the complex interplay between foreground objects and background scenes. Following the principle of Affordance, we define the affordance-aware object insertion task, which aims to seamlessly insert any object into any scene with various position prompts. To address the limited data issue and incorporate this task, we constructed the SAM-FB dataset, which contains over 3 million examples across more than 3,000 object categories. Furthermore, we introduce a strong baseline: a **Mask-Aware Dual Diffusion (MADD)** model, which utilizes a dual-stream architecture to simultaneously denoise the

RGB image and the insertion mask. By explicitly modeling the insertion mask in the diffusion process, MADD effectively facilitates the notion of affordance. Experimental results show that our method outperforms the state-of-the-art methods and exhibits strong generalization performance on in-the-wild images. Please refer to our code on <https://github.com/KaKituken/affordance-aware-any>.

1. Introduction

In the image composition scenario, common sense guides our perception of the authenticity of synthesized images: a person cannot levitate, a water bottle needs a surface for support, and a boat should be floating in the water rather than on the ground. Deviation from such common sense often leads to semantic inconsistencies on synthesized images. From a composition perspective, the background’s semantic richness plays a pivotal role in defining the placement and characteristics of foreground objects. To better

*Equal Contribution.

†Work done while at Harvard University.

describe the influence of background semantics on the foreground, we borrow the concept of *affordance* into object-scene composition tasks. Previously, Kulal *et al.* [24] explored the concept of human affordance for image synthesis. Their work, focused on inserting humans into masked scenes, extends beyond mere color or view adjustments. To generalize the setting to arbitrary object-scene synthesis, we term the new task *Affordance-Aware Object Insertion*. This task challenges models to identify suitable locations and make necessary adjustments to foreground objects, ensuring the generated images adhere to physical laws.

This work aims to build a foundation model for affordance-aware object insertion, which can put any object into any scene as shown in Figure 1. There are three primary challenges involved. First, the model must accurately recognize the appropriate affordance relationship between a background and the foreground object to be inserted. Adjustments to the inserted foreground object is crucial for achieving the intended semantic consistency. The second challenge lies in the model’s ability to generalize across a diverse range of foreground objects. Previous generative image editing methods, such as textual inversion [12], DreamBooth [43], and DreamEdit [27], are subject-specific thus hard to generalize. Our goal is to train a model that can generalize to any object. Third, our model should support a variety of input prompts for users to specify insertion locations, ranging from sparse formats like points and bounding boxes to dense masks. Moreover, in the absence of explicit prompts, the model can autonomously determine appropriate insertion locations by analyzing the semantic content of both the background and foreground.

We address these challenges through three components: **task**, **data**, and **model**. Extending the concept of *affordance* beyond Kulal *et al.*’s initial scope [24], the task of affordance-aware object insertion aims to place an arbitrary object into any scene, accommodating different positional prompts, even in the absence of explicit positional cues. It has significant implications for applications such as automated dataset synthesis. To support this task, a large-scale dataset is necessary. Existing image composition datasets, such as DreamEditBench [27], are limited in terms of the diversity of foreground object categories and the number of training samples. To overcome these limitations, we curate a new dataset called SAM-FB which is derived from SA-1B [23] for affordance learning. SAM-FB contains a variety of foreground object categories and over 3 million samples. With SAM-FB, we further introduce a strong baseline: a **Mask-Aware Dual Diffusion (MADD)** model to utilize the large-scale data, which is a diffusion-based framework that facilitates the seamless integration of diverse objects into any scene. During the denoising procedure, object position is progressively refined while the target RGB image is synthesized simultaneously, ensuring accurate alignment

between objects and positions to achieve affordance-aware insertion. Furthermore, we present a unified representation for sparse and dense prompts, enabling our model to effectively respond to various types of position inputs.

The contributions of this work are as follows:

- We introduce affordance-aware object insertion, extending object-scene composition with affordance guidance to enable realistic insertions across diverse prompts.
- We present SAM-FB, a large-scale dataset with over 3 million samples spanning diverse object categories to support affordance-aware insertion.
- We propose a strong baseline model with a dual-stream architecture that denoises object appearance and the insertion mask, facilitating affordance learning.

2. Related Work

Affordance. J.J. Gibson [3] first introduces the concept of affordance, then a series of papers [4, 11, 15, 29] dug into this concept and brought it into the image synthesis. Initially grounded in psychology, the concept emphasizes that an object’s appearance should correspond with its utilitarian aspects as perceived by humans. Further exploration within the field of image synthesis involved adjusting the orientation and gestures of generated human figures to align with their background. Therefore, prior work primarily focuses on the interaction between humans and objects [13, 51, 54] or the human-scene relationship [7, 10, 48]. Kulal *et al.* [24] made progress by introducing a model trained on person movement video data for placing people within scenes and adjusting its pose according to the surroundings. However, their model’s scope was limited to human figures. Despite these advancements, the concept of ”affordance” in image composition, which encompasses the positioning, viewing angle, and color harmony of objects within scenes, has remained relatively unexplored. Our work offers a generalized and versatile solution for object-scene composition.

Image Editing. Image editing aims to modify existing images using generative models. Generally, image editing can be divided into semantic editing (*e.g.* adding or removing objects, changing the background), style editing (*e.g.* altering color or texture), and structural editing (*e.g.* changing object size or viewpoint). By utilizing generative models like GANs [14] or Diffusion [8], users can edit image content by providing instructions and multi-modal prompts. For instance, InstructPix2Pix [5] and MoEController [26] allow semantic and style editing through text-based instructions provided by users, while Imagen Editor [47] enables more precise control of edit locations by accepting user-provided masks for the areas to be edited. Additionally, other image editing models, such as TF-ICON [35] and ImageBrush [50], accept reference images from users, con-

Model	Task	Dataset	Sample	Category	Affordance Consistency
● [27]	Customized Image Composition	DreamEditBench	440	22	High (Real Paired)
● [34]	Customized Image Composition	MureCom	640	32	High (Real Paired)
● [49], ● [44]	Image-guidance Object Insertion	Open-Images-v4	1.9M	600	Low (Masked)
● [30]	Image-guidance Object Insertion	COCO2014	165K	80	Low (Masked)
● [24]	Human Affordance Insertion	Private	2.4M	1	High (Video)
MADD (ours)	Object Affordance Insertion	SAM-FB	3.2M	3,439	High (Inpainted)

Table 1. Dataset choice and comparison. We inspect various potential datasets for affordance insertion. SAM-FB contains significantly more samples and object categories. ● DreamEdit, ● DreamCom, ● PBE, ● ObjectStitch, ● GLIGEN, ● Human Affordance.

straining the appearance of objects during editing.

Image Composition. Image composition is a sub-task within image editing, primarily focused on controllably inserting foreground objects into a background based on reference images. Recently, the utilization of generative models empowers high-quality and controllable image composition. Diffusion models have been successfully applied in various domains, including image composition [33, 44], video generation [18], and data augmentation [46]. Stable Diffusion (SD) [42] introduced methods for blending feature and semantic information from images and text, enabling object generation based on prompt instructions. Inpainting [2] is a common approach to achieve image composition. SD-based inpainting models [28, 36, 52] allow users to repaint a specific region with a mask, but it’s hard to insert a desired object into that region. Blended Diffusion [1] enables finer control by leveraging text descriptions of the foreground, but it’s crucial for user to describe the foreground precisely. PBE [49], ObjectStitch [44], and GLI-GEN [30] utilize reference images to incorporate rich visual information, achieving better perspective and color harmony. However, these models require users to provide precise positional cues, such as bounding boxes or masks, to indicate the insertion location. Our proposed method offers a viable solution for handling vague positional information, such as point prompts or even blank prompts.

3. Dataset

Instead of manually designing affordance, we use a data-driven approach to extract affordance relationships between the object and background from the large-scale dataset.

3.1. Motivation & Design Decisions

To support affordance-aware object insertion across various objects and scenes, the dataset must provide rich contextual information and extensive coverage and preserve natural affordance cues between objects and their surroundings. Therefore, we designed the dataset with the following key characteristics: 1) Well-aligned input-output pairs. Rather than using techniques like DreamBooth [43] to memorize each object individually, we adopted supervised

fine-tuning to directly learn from large-scale object distributions. Consequently, well-aligned input-output pairs, represented as (f, b, p, x) tuples, are essential. Here, f , b , p , and x denote the foreground image, background image, position prompt, and ground truth image, respectively. 2) Sufficient training samples. Training a model capable of generalizing to diverse scenarios requires a substantial number of training samples. 3) A wide variety of foreground objects. The dataset must encompass a diverse range of foreground objects to ensure that the trained model can generalize across different object categories. However, existing datasets either lack sufficient object diversity or introduce artifacts that disrupt these affordance relationships.

The (f, b, p, x) -formatted data can be derived from multiple datasets relevant to this task, as shown in Table 1. One option is to use datasets designed for Customized Image Composition. Datasets such as DreamEditBench [27] and MureCom [34] are manually captured by placing the same foreground object in different backgrounds under controlled camera settings. However, the cost of constructing such high-quality paired datasets is substantial, resulting in relatively small dataset sizes. Referring to the Image-Guided Object Insertion task, another approach is to leverage large-scale object detection datasets such as COCO [31] and Open-Images [25] to simulate foreground-background pairs. This is achieved by using bounding boxes as position prompts and extracting foreground objects from the original image using masks, treating the remaining portion as the background. However, these datasets are still insufficient to guarantee robust generalization, particularly due to their limited object category diversity. Moreover, masking out the foreground leaves an opaque region in the background, which disrupts affordance relationships. For HumanAffordance [24], they use a vast number of human-centered video to capture the affordance relationship, but the category is human only and the dataset is private. To address these limitations and obtain a sufficient number of training samples while ensuring diversity in foreground objects, we turned to the SA-1B dataset [23], which consists of 11 million high-quality images collected from various real-world scenes and 1 billion well-annotated class-agnostic masks. Based on

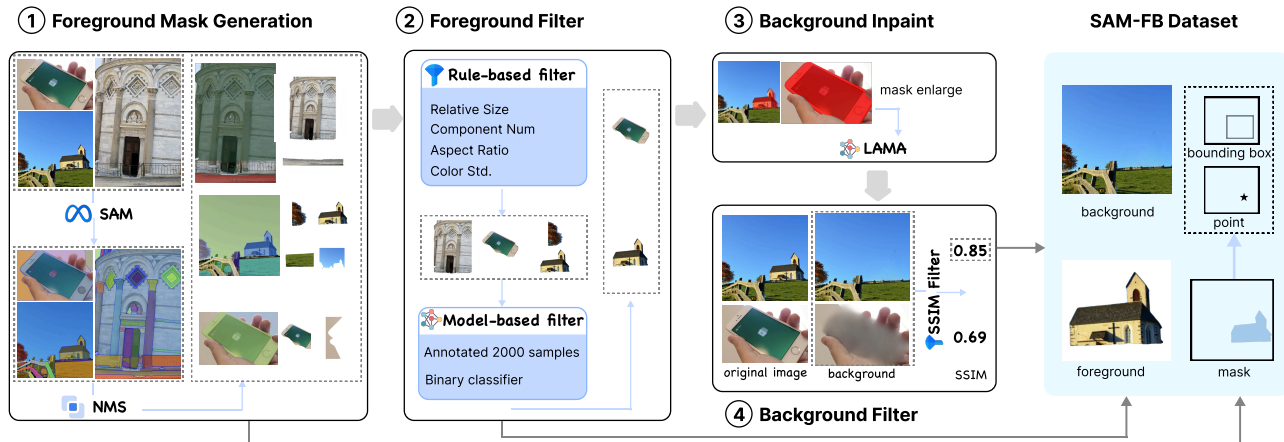


Figure 2. Dataset construction pipeline for SAM-FB. The pipeline automatically converts any input image into a tetrad output through four stages, ensuring high-quality foreground and background retention via a rigorous data quality control process.

Filter condition	Threshold	Reserved Percentage
None (Initial)	–	100%
Relative Size	[0.1, 0.75]	7.10%
Aspect Ratio	≤ 3	6.88%
Components Num.	≤ 4	6.71%
Color Std.	≥ 45	1.69%
ResNet50 Score	≥ 0.7	0.25%

Table 2. Reserved percentages for foreground quality control filters. We apply a combination of rule-based and learning-based conditions to ensure high-quality foreground objects are retained through a rigorous filtering process.

SA-1B, we constructed the SAM-FB benchmark dataset for the affordance-aware object insertion task.

3.2. Dataset Construction Pipeline

Figure 2 illustrates the pipeline used to construct the aforementioned (f, b, p, x) formatted data. The pipeline automatically transforms any input image into a tetrad output. To enhance affordance representation and improve the overall quality of the SAM-FB dataset, the dataset construction process consists of four key stages.

Foreground Mask Generation. For each unannotated input image, we first apply the Segment Anything Model (SAM) to generate object masks as candidates. Since SAM produces masks at different levels of granularity with varying confidence scores, we perform Non-Maximum Suppression (NMS) with a high threshold (0.6) to remove redundant masks and filter out sub-object-level masks. The remaining masks are used to extract candidate foreground objects.

Foreground Filtering. Although NMS removes some low-quality masks, SAM segmentation can still produce unintended elements due to challenges in controlling granularity and semantic consistency. The resulting masks often suffer from three main issues: Incompleteness: Some objects are partially occluded, resulting in fragmented masks that only

capture small portions of the original object (e.g., half of a tree); Background Masks: Some masks mistakenly segment background elements (e.g., sky, grassland); Undersized / Oversized Objects: Very small objects often have blurry details, reducing dataset quality. To enhance foreground quality, we employ a hybrid quality control (QC) approach combining rule-based and learning-based filtering.

For rule-based filtering, we remove low-quality masks with four constraints: relative size (too small/large objects), aspect ratio (overly thin objects), component count (disjointed objects), and color standard deviation (pure-color backgrounds). While rule-based filtering effectively removes outliers, ensuring object completeness is challenging using predefined rules alone. To address this, we manually annotate 2,000 foreground images with binary labels (good vs. bad) and fine-tune a ResNet-50 [16] classifier for binary classification. The trained classifier assigns a quality score to each foreground object, further refining the dataset. Table 2 demonstrates the specific threshold for each filter operation of our data quality control stage. With these filter operations, only 0.25% of the masks are left, which ensures the quality of the obtained dataset.

Background Inpainting. High-quality foregrounds are then cropped from the original images. Instead of covering the removed regions with opaque masks, which act as strong artificial cues for object position and size, we employ LAMA [45] for background inpainting. LAMA is a simple yet effective method for object removal and hole-filling. Following GroundingSAM [32, 41], we expand the object mask boundary slightly to prevent residual foreground content from remaining in the background. By eliminating such visual cues, our dataset encourages models to infer context-aware object placement based on scene affordances.

Background Inpainting. Despite careful inpainting, some regions inevitably contain inpainting artifacts. To assess the

quality of inpainted backgrounds, we compute the Structural Similarity Index (SSIM) between the inpainted background and the original image. We discard any inpainted background with an SSIM score below a certain threshold to maintain high visual consistency. We empirically set the SSIM threshold to 0.8 based on preliminary experiments assessing inpainting realism. If a background fails the SSIM filter, we discard the entire foreground-background pair, even if the foreground quality is high. This ensures that only high-quality samples are included in the dataset.

To evaluate quality improvements, we compute the Inception Score (IS) for foregrounds and Fréchet Inception Distance (FID) for backgrounds, comparing values before and after quality control (QC). After QC, foreground IS improves from 9.55 to 16.68, indicating significantly enhanced foreground clarity, while background FID decreases from 9.23 to 8.46, reflecting better distribution consistency, similar to inpainting tasks. Since FID requires a reference distribution, it is less meaningful for foregrounds, whereas IS is not a reliable metric for complex backgrounds. To justify the diversity of our proposed dataset, we use RAM [53] to recognize the categories of foregrounds we keep. We have identified 3439 different categories, which is a vast improvement over previous datasets. There are no manual annotations required in the pipeline, and users can easily scale up the dataset further with any new source images easily.

4. Method

4.1. Mask-Aware Dual Diffusion Model (MADD)

Preliminaries. Given a foreground object f , a background scene b , and a position prompt p , the goal is to synthesize an image x that integrates the object into the scene, while adhering to affordances and aligning with the position prompt.

To develop an effective diffusion model, we first extract image features $z = \mathcal{E}(x)$ using a pre-trained encoder. Then we predict the object insertion mask m capturing object’s location and size, which can be directly derived from the difference between x and b in the training data. Our MADD model \mathcal{G} builds upon the latent structural diffusion framework [33], simultaneously denoising \hat{z} and \hat{m} (Figure 3):

$$\hat{z}, \hat{m} = \mathcal{G}(f, b, p), \quad (1)$$

where the estimated image is reconstructed by $\hat{x} = \mathcal{D}(\hat{z})$ with the corresponding image decoder.

Forward Process. The noised feature maps are

$$z_{t_z} = \alpha_{t_z} z + \sigma_{t_z} \epsilon_{t_z}, \quad m_{t_m} = \alpha_{t_m} m + \sigma_{t_m} \epsilon_{t_m}, \quad (2)$$

where ϵ_z and $\epsilon_m \sim \mathbf{N}(0, I)$ are three independently sampled Gaussian noise, and the time step t_z and t_m are sampled from a uniform distribution $\mathcal{U}[0, 1]$.

Reverse Process. The denoiser $\hat{\epsilon}_\theta$ simultaneously denoises

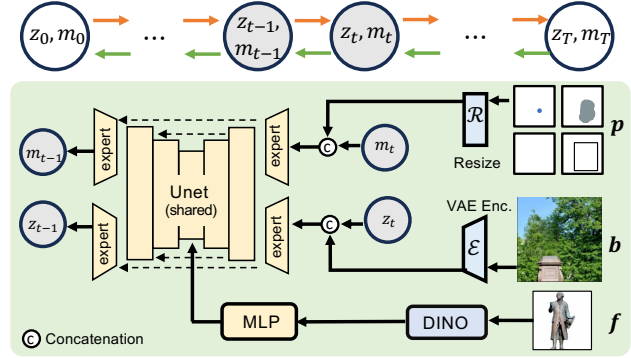


Figure 3. Mask-aware Dual Diffusion Model (MADD). The RGB image feature z and object mask m are jointly denoised, conditioning on the embeddings of the foreground object f , background object b , and the prompt p . (green: reverse process $t \rightarrow t-1$)

both z_{t_z} and m_{t_m} , which can be trained with:

$$\mathcal{L} = \mathbb{E} [\|\epsilon_z - \hat{\epsilon}_\theta(z_{t_z}; f, b, p)\|^2] + \mathbb{E} [\|\epsilon_m - \hat{\epsilon}_\theta(m_{t_m}; f, b, p)\|^2].$$

The denoiser model consists of the UNet model and the three encoders for the foreground object f , the background scene b , and the position prompt p , respectively.

4.2. Architecture Details

UNet Model. We utilize a single UNet with two expert input-output branches to denoise them simultaneously. The two tasks share the entire UNet except for the `conv_in`, first `Down Block`, last `Up Block`, and the `conv_out`. These independent blocks serve as the Expert input-output branch. Skip connection is also performed between the corresponding Expert input and output branches.

Foreground Encoder. In MADD, foreground images serve as a guidance condition and are incorporated into the model via cross-attention. The foreground embedding is extracted using a ViT-like visual encoder. While SD employs the CLIP [40] encoder for text-aligned semantics, we follow Efficient-3DiM [20] and use DINOv2 [37] to preserve fine-grained object details, making it more suitable for our task.

Background Encoder. Following SD-based image editing methods [5, 44], we employ a pre-trained VAE encoder to convert the background image into a 4-channel latent representation. Since the background is pixel-aligned with the output, we concatenate its latent map with z_t before feeding them into the U-Net. The pre-trained VAE decoder then reconstructs the final RGB image from the latent output.

Position Prompt Encoder. We design a unified representation to process different position prompts. Sparse and dense prompts are converted into a 1-channel position map, guiding foreground object placement. Point prompts are transformed into Gaussian heatmaps, bounding boxes are filled with ones inside and zeros outside, and masks are binary

Method	FID↓		CLIP Score↑		MSE↓	
	mask	bbox	mask	bbox	mask	bbox
🟡 [42]	15.41	15.47	0.7079	0.8058	860	883
🟠 [49]	33.68	24.59	-	0.7664	2373	1615
🟢 [30]	-	13.82	-	0.7896	-	817
🟣 [24]	14.49	14.42	0.8014	0.8637	857	845
Ours	13.53	13.60	0.8727	0.8658	760	775

Table 3. Method comparisons on the SAM-FB test set. 🟡 Stable Diffusion, 🟠 PBE, 🟢 GLIGEN, 🟣 Human Affordance.

Prompt	Mask	Bbox	Point	Null	Avg.
FID	13.53	13.60	13.66	13.96	13.69
MSE	760	775	772	860	792
CLIP Score	0.8727	0.8658	0.8567	0.8034	0.8497

Table 4. Comparison of position prompts on the SAM-FB test set.

maps. For null prompts, an all-one image implies all positions are possible. The position map is resized to match the latent map’s spatial dimensions and concatenated with it before being fed into the diffusion U-Net.

4.3. Implementation Details

We initialize our model with a pre-trained Stable Diffusion Inpainting model and apply strong data augmentation to enhance affordance learning. To optimize fine-tuning, we use a coarse-to-fine strategy: training at 128×128 resolution (batch size 1024) for 35K steps, then fine-tuning at 256×256 (batch size 256) for 15K steps.

5. Experiments

5.1. Results on the SAM-FB Test Set

Evaluation Metrics. Following the previous work [6, 19, 22, 35], we employ the FID score to measure the quality of images obtained by generative models, MSE for pixel similarity and the CLIP score to evaluate the semantic similarity between the edited region and the reference foreground.

Quantitative Results. We compare our method with Stable Diffusion [42], PBE [49], GLI-GEN [30], and Human Affordance [24] on the SAM-FB test set to show the effectiveness of our method. For fairness, we fine-tuned GLI-GEN [28] on SAM-FB training data for 2k steps with captions generated by ViT-GPT2 [9, 39] and use Box + Text + Image Inpainting mode to adapt it. Since Human Affordance [24] does not release training data or model weights, we re-trained their model on SAM-FB. The results in Table 3 show that our method attains the best FID score and the highest CLIP score, illustrating our model can be a simple yet strong baseline for affordance-aware object insertion task. Table 4 shows that the mask prompt achieves the best results as it provides more accurate position information.

Qualitative Results. We left 3786 images as test split. Fig-

Prompt	Non-Null	Null
IoU (↑)	0.5405	0.4696

Table 5. Mask evaluation

Model Components		
Method	FID (↓)	CLIP (↑)
Baseline	18.32	0.79
+ Dual diffusion	14.43	0.84
+ Expert branch	13.69	0.85
Higher Resolution		
256×256	13.69	0.85
512×512	10.66	0.82

Table 6. Ablation study results on SAM-FB test set.

ure 4 presents the visualization results on the SAM-FB test set. In each group, the leftmost image depicts the background marked with a position prompt. Our MADD predicts the RGB image and mask of the inserted object, which are shown in the last two images of each group. These results demonstrate that MADD not only inserts objects with high quality but also accurately predicts object masks.

Mask Evaluation. Table 5 shows the IoU of the mask between the predicted mask and the ground truth on the SAM-FB test set. The relatively high IoU shows that our method learns effective affordance information.

Computational complexity. We access the computational complexity for the newly added modules including Dual Diffusion and Expert Branch. Using Human Affordance model with DINOv2 as baseline, it has 863.02M parameters with 28.3B FLOPs. Our Expert branches shared most of the parameters with the original baseline model and end up with 873.75M parameters with 31.1B FLOPs.

5.2. Ablation Studies

Model Components. Table 6 presents the results of our ablation study. For model design, we replace the image encoder in the Human Affordance model with DINOv2 as the baseline. Next, we diffuse RGB image and object mask simultaneously, but sharing the entire UNet. Finally, we use two Expert branches for mask and RGB streams. The results show that all of them improved performance. Metrics are averaged across different position prompts. Please refer to the supplementary for results on each prompt type.

Higher Resolution. Even though we trained our model at a resolution of 256×256 , it is also capable of handling higher-resolution inputs, such as 512×512 . To prove that, we then fine-tuned our model on SAM-FB at a resolution of 512×512 for only 200 steps and compared it with the original checkpoint on the test split. Figure 6 shows the results of the original checkpoint and the fine-tuned version at higher resolution using the same input. We highlighted the details of the inserted object. It is clearly demonstrated that the

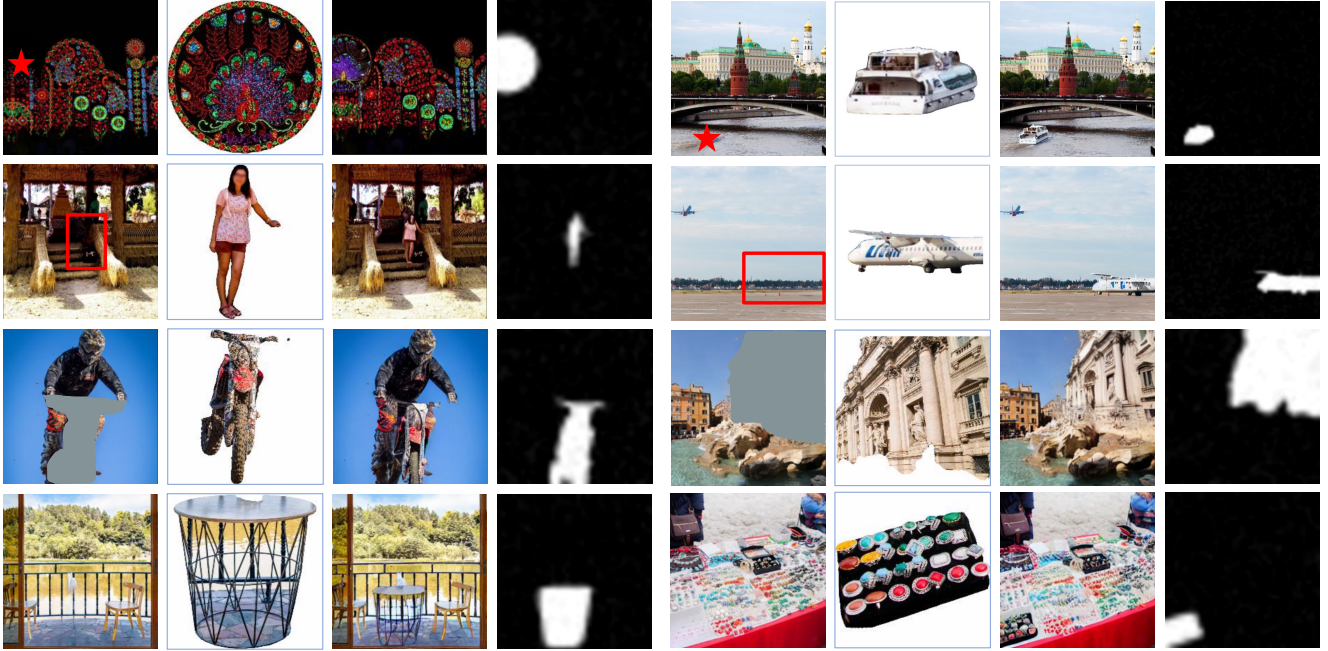


Figure 4. Qualitative results of MADD on the SAM-FB test set. Each row corresponds to one type of prompt, *i.e.*, point, bounding box, mask, and null, respectively. Our MADD simultaneously predicts the RGB image and the object mask.



Figure 5. We test ambiguous prompts (points and blank) on in-the-wild images. With point prompts, our model adjusts foreground properties for affordance-aware insertion, while it autonomously finds suitable positions when no prompt is given.

model generates sharper edges, clearer reflections, and improved texture details after fine-tuning at higher resolution. The CLIP score drops slightly at 512×512, likely due to the increased complexity of higher-resolution foregrounds, making fine-grained detail synthesis more challenging.

5.3. Results on In-the-wild Images

We evaluate our model on in-the-wild web-crawled images. **Ambiguous Prompts.** Training with position augmentations enables the model to capture affordance relationships between objects and scenes. MADD refines object position, size, and view for coherence with the background.

In Figure 5, MADD adjusts a person’s position to stand on the ground rather than floating, aligns a car’s orientation with the lane, and scales coffee beans to match the scene. The model can also place objects without explicit prompts and generate diverse, reasonable insertions based on user input and learned affordance, as shown in Figure 7.

Human Evaluation. To test the generalization ability of our MADD model, we performed affordance insertion on

in-the-wild images and compared the results with Stable Diffusion XL [38], GLI-GEN [30], PBE [49] and Object-Stitch [44]. Instead of merely relying on metrics like FID and CLIP Score, we also conducted user study to achieve more comprehensive comparison. We asked 10 users to rank 10 groups of composited image generated from from different model according to the following criteria: 1) Foreground and Background Integration; 2) Foreground Clarity and Detail; 3) Foreground Appearance Consistency with Reference; 4) Lighting and shade on Foreground; 5) Color Consistency. Figure 8 shows the distribution of rank for different models, where rank 1 and rank 5 represent the best and worst quality respectively. Our model achieves 50% of Rank-1 place and 1.60% of the Rank-5 place, which outperforms other methods. Please refer to supplementary for details of each criteria. Our model consistently achieved the highest proportion of Rank-1 placements across all evaluation criteria, as indicated by the largest segments in each pie chart. Especially for keeping the consistency of foreground appearance with reference image. This dominance in Rank-



Figure 6. MADD can work on images of higher resolution, generating sharper edges, clearer reflections, improved texture details.

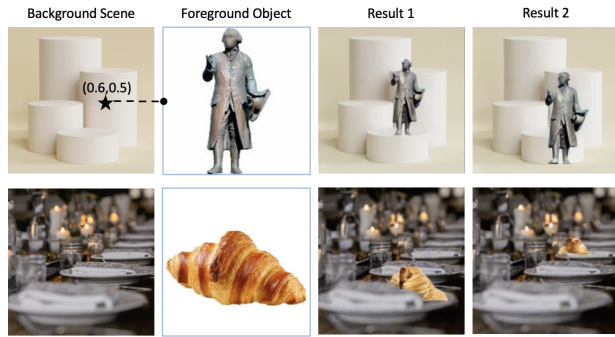


Figure 7. MADD can give different feasible solutions for ambiguous prompts such as point and blank.

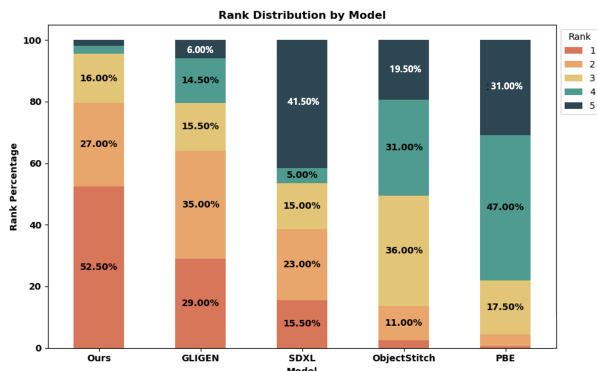


Figure 8. Rank distribution for different methods. Our method has the most proportion of rank 1 and least proportion of rank 5.

1 distribution across multiple criteria highlights the model’s superior performance compared to others in all aspects.

More Results. Figure 9 presents additional in-the-wild examples of affordance-aware object insertion with various position prompts. For ambiguous prompts, such as points or null inputs, MADD infers a reasonable position and adjusts the foreground accordingly. For bounding boxes and



Figure 9. More in-the-wild affordance-insertion examples. The model can generate an affordance-feasible solution to insert the foreground objects according to the background scene.

masks, MADD treats them as guidance rather than strict constraints, refining placements to ensure coherence. Please refer to the supplementary for additional examples that further demonstrate MADD’s ability to generate suitable and diverse insertions in real-world scenarios.

6. Conclusion

In this paper, we extend the concept of affordance beyond human-centered tasks by introducing affordance-aware object insertion, enabling seamless object placement into scenes while adhering to affordance principles. To support this, we construct SAM-FB, a dataset of 3.16 million foreground-background pairs spanning 3,000+ object categories. We propose MADD, a dual-stream diffusion model that jointly denoises foreground appearance and object masks, leveraging affordance relationships for context-aware insertion. MADD accommodates various position prompts and can infer placements autonomously. Our model generalizes well across diverse objects and outperforms prior diffusion-based composition methods, achieving coherent and affordance-aware insertions.

References

- [1] Omri Avrahami, Dani Lischinski, and Ohad Fried. Blended diffusion for text-driven editing of natural images. In *Proceedings of the IEEE/CVF Conference on Computer Vision and Pattern Recognition*, pages 18208–18218, 2022. 3
- [2] Marcelo Bertalmio, Guillermo Sapiro, Vincent Caselles, and Coloma Ballester. Image inpainting. In *Proceedings of the 27th annual conference on Computer graphics and interactive techniques*, pages 417–424, 2000. 3
- [3] Marc H Bornstein. The ecological approach to visual perception, 1980. 2
- [4] Tim Brooks and Alexei A Efros. Hallucinating pose-compatible scenes. In *European Conference on Computer Vision*, pages 510–528. Springer, 2022. 2
- [5] Tim Brooks, Aleksander Holynski, and Alexei A Efros. Instructpix2pix: Learning to follow image editing instructions. In *Proceedings of the IEEE/CVF Conference on Computer Vision and Pattern Recognition*, pages 18392–18402, 2023. 2, 5
- [6] Guillaume Couairon, Jakob Verbeek, Holger Schwenk, and Matthieu Cord. Diffedit: Diffusion-based semantic image editing with mask guidance. *arXiv preprint arXiv:2210.11427*, 2022. 6
- [7] Vincent Delaitre, David F Fouhey, Ivan Laptev, Josef Sivic, Abhinav Gupta, and Alexei A Efros. Scene semantics from long-term observation of people. In *Computer Vision—ECCV 2012: 12th European Conference on Computer Vision, Florence, Italy, October 7–13, 2012, Proceedings, Part VI 12*, pages 284–298. Springer, 2012. 2
- [8] Prafulla Dhariwal and Alexander Nichol. Diffusion models beat gans on image synthesis. *Advances in neural information processing systems*, 34:8780–8794, 2021. 2
- [9] Alexey Dosovitskiy, Lucas Beyer, Alexander Kolesnikov, Dirk Weissenborn, Xiaohua Zhai, Thomas Unterthiner, Mostafa Dehghani, Matthias Minderer, Georg Heigold, Sylvain Gelly, et al. An image is worth 16x16 words: Transformers for image recognition at scale. *arXiv preprint arXiv:2010.11929*, 2020. 6
- [10] David F Fouhey, Vincent Delaitre, Abhinav Gupta, Alexei A Efros, Ivan Laptev, and Josef Sivic. People watching: Human actions as a cue for single view geometry. In *Computer Vision—ECCV 2012: 12th European Conference on Computer Vision, Florence, Italy, October 7–13, 2012, Proceedings, Part V 12*, pages 732–745. Springer, 2012. 2
- [11] David F Fouhey, Xiaolong Wang, and Abhinav Gupta. In defense of the direct perception of affordances. *arXiv preprint arXiv:1505.01085*, 2015. 2
- [12] Rinon Gal, Yuval Alaluf, Yuval Atzmon, Or Patashnik, Amit H Bermano, Gal Chechik, and Daniel Cohen-Or. An image is worth one word: Personalizing text-to-image generation using textual inversion. *arXiv preprint arXiv:2208.01618*, 2022. 2
- [13] Georgia Gkioxari, Ross Girshick, Piotr Dollár, and Kaiming He. Detecting and recognizing human-object interactions. In *Proceedings of the IEEE conference on computer vision and pattern recognition*, pages 8359–8367, 2018. 2
- [14] Ian Goodfellow, Jean Pouget-Abadie, Mehdi Mirza, Bing Xu, David Warde-Farley, Sherjil Ozair, Aaron Courville, and Yoshua Bengio. Generative adversarial nets. *Advances in neural information processing systems*, 27, 2014. 2
- [15] Abhinav Gupta, Scott Satkin, Alexei A Efros, and Martial Hebert. From 3d scene geometry to human workspace. In *CVPR 2011*, pages 1961–1968. IEEE, 2011. 2
- [16] Kaiming He, Xiangyu Zhang, Shaoqing Ren, and Jian Sun. Deep residual learning for image recognition. In *Proceedings of the IEEE conference on computer vision and pattern recognition*, pages 770–778, 2016. 4
- [17] Jonathan Ho and Tim Salimans. Classifier-free diffusion guidance. *arXiv preprint arXiv:2207.12598*, 2022. 1
- [18] Jonathan Ho, Tim Salimans, Alexey Gritsenko, William Chan, Mohammad Norouzi, and David J Fleet. Video diffusion models. *Advances in Neural Information Processing Systems*, 35:8633–8646, 2022. 3
- [19] Hyeonho Jeong, Gihyun Kwon, and Jong Chul Ye. Zero-shot generation of coherent storybook from plain text story using diffusion models. *arXiv preprint arXiv:2302.03900*, 2023. 6
- [20] Yifan Jiang, Hao Tang, Jen-Hao Rick Chang, Liangchen Song, Zhangyang Wang, and Liangliang Cao. Efficient-3dim: Learning a generalizable single-image novel-view synthesizer in one day. *arXiv preprint arXiv:2310.03015*, 2023. 5
- [21] Tero Karras, Miika Aittala, Janne Hellsten, Samuli Laine, Jaakko Lehtinen, and Timo Aila. Training generative adversarial networks with limited data. *Advances in neural information processing systems*, 33:12104–12114, 2020. 1
- [22] Bahjat Kawar, Shiran Zada, Oran Lang, Omer Tov, Huiwen Chang, Tali Dekel, Inbar Mosseri, and Michal Irani. Imagic: Text-based real image editing with diffusion models. In *Proceedings of the IEEE/CVF Conference on Computer Vision and Pattern Recognition*, pages 6007–6017, 2023. 6
- [23] Alexander Kirillov, Eric Mintun, Nikhila Ravi, Hanzi Mao, Chloe Rolland, Laura Gustafson, Tete Xiao, Spencer Whitehead, Alexander C Berg, Wan-Yen Lo, et al. Segment anything. *arXiv preprint arXiv:2304.02643*, 2023. 2, 3
- [24] Sumith Kulal, Tim Brooks, Alex Aiken, Jiajun Wu, Jimei Yang, Jingwan Lu, Alexei A Efros, and Krishna Kumar Singh. Putting people in their place: Affordance-aware human insertion into scenes. In *Proceedings of the IEEE/CVF Conference on Computer Vision and Pattern Recognition*, pages 17089–17099, 2023. 2, 3, 6, 1
- [25] Alina Kuznetsova, Hassan Rom, Neil Alldrin, Jasper Uijlings, Ivan Krasin, Jordi Pont-Tuset, Shahab Kamali, Stefan Popov, Matteo Mallocci, Alexander Kolesnikov, et al. The open images dataset v4: Unified image classification, object detection, and visual relationship detection at scale. *International Journal of Computer Vision*, 128(7):1956–1981, 2020. 3
- [26] Sijia Li, Chen Chen, and Haonan Lu. Moecontroller: Instruction-based arbitrary image manipulation with mixture-of-expert controllers. *arXiv preprint arXiv:2309.04372*, 2023. 2
- [27] Tianle Li, Max Ku, Cong Wei, and Wenhui Chen. Dreamedit: Subject-driven image editing. *arXiv preprint arXiv:2306.12624*, 2023. 2, 3

- [28] Wenbo Li, Zhe Lin, Kun Zhou, Lu Qi, Yi Wang, and Jiaya Jia. Mat: Mask-aware transformer for large hole image inpainting. In *Proceedings of the IEEE/CVF conference on computer vision and pattern recognition*, pages 10758–10768, 2022. 3
- [29] Xueting Li, Sifei Liu, Kihwan Kim, Xiaolong Wang, Ming-Hsuan Yang, and Jan Kautz. Putting humans in a scene: Learning affordance in 3d indoor environments. In *Proceedings of the IEEE/CVF Conference on Computer Vision and Pattern Recognition*, pages 12368–12376, 2019. 2
- [30] Yuheng Li, Haotian Liu, Qingyang Wu, Fangzhou Mu, Jianwei Yang, Jianfeng Gao, Chunyuan Li, and Yong Jae Lee. Gligen: Open-set grounded text-to-image generation. In *Proceedings of the IEEE/CVF Conference on Computer Vision and Pattern Recognition*, pages 22511–22521, 2023. 3, 6, 7, 4
- [31] Tsung-Yi Lin, Michael Maire, Serge Belongie, James Hays, Pietro Perona, Deva Ramanan, Piotr Dollár, and C Lawrence Zitnick. Microsoft coco: Common objects in context. In *Computer Vision—ECCV 2014: 13th European Conference, Zurich, Switzerland, September 6–12, 2014, Proceedings, Part V 13*, pages 740–755. Springer, 2014. 3
- [32] Shilong Liu, Zhaoyang Zeng, Tianhe Ren, Feng Li, Hao Zhang, Jie Yang, Chunyuan Li, Jianwei Yang, Hang Su, Jun Zhu, et al. Grounding dino: Marrying dino with grounded pre-training for open-set object detection. *arXiv preprint arXiv:2303.05499*, 2023. 4
- [33] Xian Liu, Jian Ren, Aliaksandr Siarohin, Ivan Skorokhodov, Yanyu Li, Dahua Lin, Xihui Liu, Ziwei Liu, and Sergey Tulyakov. Hyperhuman: Hyper-realistic human generation with latent structural diffusion. *arXiv preprint arXiv:2310.08579*, 2023. 3, 5
- [34] Lingxiao Lu, Bo Zhang, and Li Niu. Dreamcom: Finetuning text-guided inpainting model for image composition. *arXiv preprint arXiv:2309.15508*, 2023. 3
- [35] Shilin Lu, Yanzhu Liu, and Adams Wai-Kin Kong. Tf-icon: Diffusion-based training-free cross-domain image composition. In *Proceedings of the IEEE/CVF International Conference on Computer Vision*, pages 2294–2305, 2023. 2, 6
- [36] Andreas Lugmayr, Martin Danelljan, Andres Romero, Fisher Yu, Radu Timofte, and Luc Van Gool. Repaint: Inpainting using denoising diffusion probabilistic models. In *Proceedings of the IEEE/CVF Conference on Computer Vision and Pattern Recognition*, pages 11461–11471, 2022. 3
- [37] Maxime Oquab, Timothée Darcet, Théo Moutakanni, Huy Vo, Marc Szafraniec, Vasil Khalidov, Pierre Fernandez, Daniel Haziza, Francisco Massa, Alaaeldin El-Nouby, et al. Dinov2: Learning robust visual features without supervision. *arXiv preprint arXiv:2304.07193*, 2023. 5
- [38] Dustin Podell, Zion English, Kyle Lacey, Andreas Blattmann, Tim Dockhorn, Jonas Müller, Joe Penna, and Robin Rombach. Sdxl: Improving latent diffusion models for high-resolution image synthesis. *arXiv preprint arXiv:2307.01952*, 2023. 7
- [39] Alec Radford, Jeff Wu, Rewon Child, David Luan, Dario Amodei, and Ilya Sutskever. Language models are unsupervised multitask learners. 2019. 6
- [40] Alec Radford, Jong Wook Kim, Chris Hallacy, Aditya Ramesh, Gabriel Goh, Sandhini Agarwal, Girish Sastry, Amanda Askell, Pamela Mishkin, Jack Clark, et al. Learning transferable visual models from natural language supervision. In *International conference on machine learning*, pages 8748–8763. PMLR, 2021. 5
- [41] Tianhe Ren, Shilong Liu, Ailing Zeng, Jing Lin, Kunchang Li, He Cao, Jiayu Chen, Xinyu Huang, Yukang Chen, Feng Yan, et al. Grounded sam: Assembling open-world models for diverse visual tasks. *arXiv preprint arXiv:2401.14159*, 2024. 4
- [42] Robin Rombach, Andreas Blattmann, Dominik Lorenz, Patrick Esser, and Björn Ommer. High-resolution image synthesis with latent diffusion models. In *Proceedings of the IEEE/CVF conference on computer vision and pattern recognition*, pages 10684–10695, 2022. 3, 6, 4
- [43] Nataniel Ruiz, Yuanzhen Li, Varun Jampani, Yael Pritch, Michael Rubinstein, and Kfir Aberman. Dreambooth: Fine tuning text-to-image diffusion models for subject-driven generation. In *Proceedings of the IEEE/CVF Conference on Computer Vision and Pattern Recognition*, pages 22500–22510, 2023. 2, 3
- [44] Yizhi Song, Zhifei Zhang, Zhe Lin, Scott Cohen, Brian Price, Jianming Zhang, Soo Ye Kim, and Daniel Aliaga. Object-stitch: Object compositing with diffusion model. In *Proceedings of the IEEE/CVF Conference on Computer Vision and Pattern Recognition*, pages 18310–18319, 2023. 3, 5, 7
- [45] Roman Suvorov, Elizaveta Logacheva, Anton Mashikhin, Anastasia Remizova, Arsenii Ashukha, Aleksei Silvestrov, Naejin Kong, Harshith Goka, Kiwoong Park, and Victor Lempitsky. Resolution-robust large mask inpainting with fourier convolutions. *arXiv preprint arXiv:2109.07161*, 2021. 4
- [46] Brandon Trabucco, Kyle Doherty, Max Gurinas, and Ruslan Salakhutdinov. Effective data augmentation with diffusion models. *arXiv preprint arXiv:2302.07944*, 2023. 3
- [47] Su Wang, Chitwan Saharia, Ceslee Montgomery, Jordi Pont-Tuset, Shai Noy, Stefano Pellegrini, Yasumasa Onoe, Sarah Laszlo, David J Fleet, Radu Soricut, et al. Imagen editor and editbench: Advancing and evaluating text-guided image inpainting. In *Proceedings of the IEEE/CVF conference on computer vision and pattern recognition*, pages 18359–18369, 2023. 2
- [48] Xiaolong Wang, Rohit Girdhar, and Abhinav Gupta. Binge watching: Scaling affordance learning from sitcoms. In *Proceedings of the IEEE Conference on Computer Vision and Pattern Recognition*, pages 2596–2605, 2017. 2
- [49] Binxin Yang, Shuyang Gu, Bo Zhang, Ting Zhang, Xuejin Chen, Xiaoyan Sun, Dong Chen, and Fang Wen. Paint by example: Exemplar-based image editing with diffusion models. In *Proceedings of the IEEE/CVF Conference on Computer Vision and Pattern Recognition*, pages 18381–18391, 2023. 3, 6, 7, 4
- [50] Yifan Yang, Houwen Peng, Yifei Shen, Yuqing Yang, Han Hu, Lili Qiu, Hideki Koike, et al. Imagebrush: Learning visual in-context instructions for exemplar-based image manipulation. *Advances in Neural Information Processing Systems*, 36, 2024. 2

- [51] Bangpeng Yao and Li Fei-Fei. Modeling mutual context of object and human pose in human-object interaction activities. In *2010 IEEE Computer Society Conference on Computer Vision and Pattern Recognition*, pages 17–24. IEEE, 2010. [2](#)
- [52] Jiahui Yu, Zhe Lin, Jimei Yang, Xiaohui Shen, Xin Lu, and Thomas S Huang. Generative image inpainting with contextual attention. In *Proceedings of the IEEE conference on computer vision and pattern recognition*, pages 5505–5514, 2018. [3](#)
- [53] Youcai Zhang, Xinyu Huang, Jinyu Ma, Zhaoyang Li, Zhaochuan Luo, Yanchun Xie, Yuzhuo Qin, Tong Luo, Yaqian Li, Shilong Liu, et al. Recognize anything: A strong image tagging model. *arXiv preprint arXiv:2306.03514*, 2023. [5](#)
- [54] Yuke Zhu, Alireza Fathi, and Li Fei-Fei. Reasoning about object affordances in a knowledge base representation. In *Computer Vision–ECCV 2014: 13th European Conference, Zurich, Switzerland, September 6–12, 2014, Proceedings, Part II 13*, pages 408–424. Springer, 2014. [2](#)

Affordance-Aware Object Insertion via Mask-Aware Dual Diffusion

Supplementary Material

A. More Implementation Details

A.1. SAM-FB Dataset

Figure 10a shows the object masks before and after the data quality control. We see that with our designed data quality control, the foreground object masks have better quality. Figure 10b illustrates the word cloud of our SAM-FB dataset, we observe that our SAM-FB dataset consists of diverse object categories.

A.2. Training Details

We constructed our dual-stream UNet based on the Stable Diffusion Inpainting v1.5 model, incorporating several modifications. Specifically, we replicated both the first down-sampling block (including `conv_in` and the first `Down Block`) and the last up-sampling block (including the last `Up Block` and `conv_out`) to accommodate dual-stream inputs and outputs. These independent blocks serve as the expertise input-output branch. Skip connection is also performed between the corresponding expertise input and output branches. To bypass the need to start from scratch, we initialized our model using the pre-trained Stable Diffusion Inpainting v1.5 checkpoint for the unchanged blocks. Fine-tuning is resource-intensive. To optimize our computing resources, we employed a gradual scaling-up approach to train our model. Initially, the model was trained at a resolution of 128×128 , with a batch size of 1024 and a learning rate of 1.25×10^{-4} for 35K steps on 2 A-100 GPUs. This phase included 5,000 warm-up steps, followed by a constant schedule. We then fine-tuned the model at a higher resolution of 256×256 , reducing the batch size to 256 and adjusting the learning rate to 5×10^{-5} . For the diffusion process, the time step is 1000 with a linear noise scheduler. We use 2048 samples of SAM-FB for testing and the rest for training. For each foreground object, all different position prompts p can be generated with the mask s . We apply classifier-free guidance [17], dropping all conditions with 0.1 probability. To ensure a fair comparison with other methods, we re-implemented and re-trained the closest method, Human Affordance, since the authors did not release either the model weights or the full dataset they used. We adopted the diffusion model architecture provided by the authors and trained it using our SAM-FB dataset. Additionally, we replaced the mask input in the original model with our position map to ensure compatibility with the SAM-FB dataset.

A.3. Data Augmentation

To prevent the model from learning a copy-and-paste process, we introduce different augmentations for the background images, foreground images, and position prompts.

Background Augmentation Given that the images in the SA-1B dataset are not square, we rescale and crop them focusing on the objects. Our first step is to resize each source image so that its shorter edge measures 256 pixels. Following this, we randomly center a 256×256 bounding box around each valid object mask, randomly chosen to provide varied backgrounds for the same object. This technique introduces slight background differences for identical objects. Additionally, we allow the bounding boxes to partially crop the objects. This strategy is specifically designed to enable the model to learn from scenarios where objects are partially obscured by the edges of the image.

Foreground Augmentation To prevent the model from simply copying and pasting foreground objects and to increase the diversity of foreground objects, data augmentation is necessary. We used geometric and color augmentations based on Kulal’s work [24] and StyleGAN-ADA [21]. Geometric augmentations included isotropic scaling, rotation, anisotropic scaling, and cutout, each with a probability of 0.4, 0.4, 0.2, and 0.2 respectively. Color augmentations included brightness, contrast, saturation, image-space filtering, and additive noise, each with a probability of 0.2.

Position Prompt Augmentation Our method requires the model to perceptively adjust the position of the inserted object in response to an ambiguous position prompt; therefore, it is also necessary to augment the position prompts. For points, we perform random jittering to deviate them from their original positions. For bounding boxes, we randomly enlarge each box. We adopt mask enlarging and feathering for mask prompts.

B. Evaluation

B.1. Evaluation metrics

Our method aims to establish a reasonable relationship between foreground objects and background scenes while maintaining the appearance of the object similar to a reference image and generating a high-quality synthetic image. To assess these two capabilities, we employ two metrics. Firstly, we use the FID score, which is widely used to measure the harmony of images obtained by generative models, to evaluate the quality of synthetic images. We use a pre-trained Inception model to extract features and calculate the FID score between generated images and ground truth im-

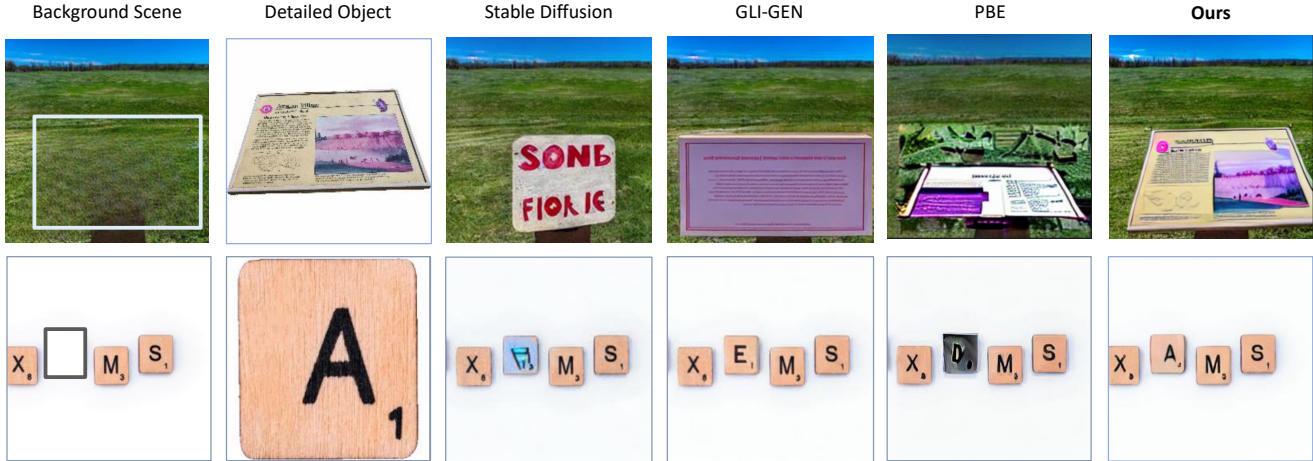


Figure 11. Example of objects with details. Our model could keep the appearance better even with some details compared with SD [42], GLI-GEN [30] and PBE [49]. The first row demonstrates the ability to keep some image texture, and the second row illustrates the ability to keep text texture.

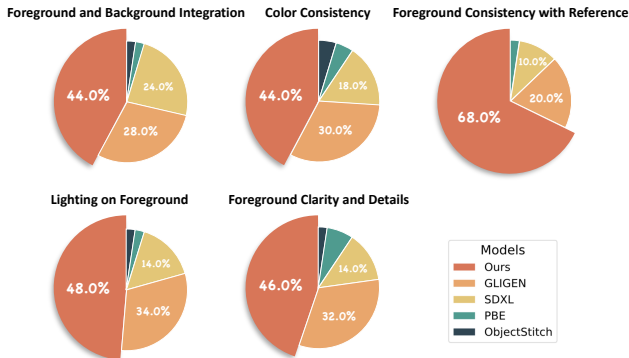


Figure 12. Rank-1 distribution for each criterion. Each pie chart represents the proportion of times each model achieved Rank-1 for a specific evaluation criterion. Our method dominates every



Figure 13. Affordance insertion away from inpainted region

Training Datasets	FID (↓)	CLIP (↑)
COCO	31.17	0.75
SAM-FB	28.45	0.77

Table 8. Ablation study results on SAM-FB test set.

SAM-FB subset, each for 10k steps, then evaluated on PascalVOC as in-the-wild benchmark. Table 8 shows SAM-FB lead to lower FID and higher CLIP score.

C.5. In-the-wild Generalization

We compare our methods with other baseline models on in-the-wild images, and Figure 15 shows the visualization results for comparison. In the first five rows, we per-

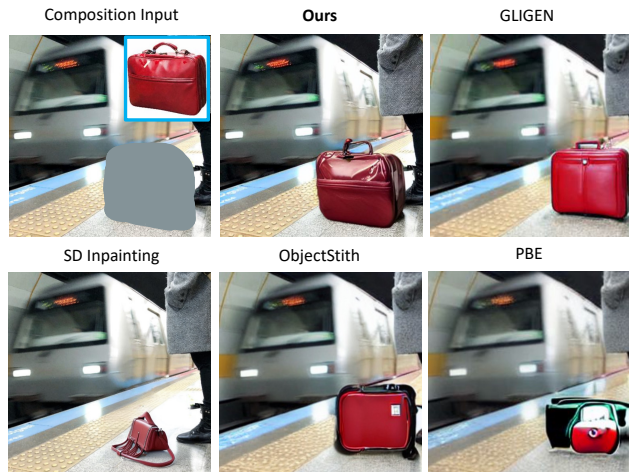


Figure 14. Samples on SAM-FB test split. Our model inserted the bag with authentic appearance.

formed affordance insertion task providing a bounding box on both common objects like apple and uncommon objects like cruta. Our methods generated the images with highest quality, authentic to the reference foreground with proper lighting. In the last row, we show more affordance insertion results when providing ambiguous prompts. The model will automatically find the proper affordance relationship and adjust the location and view of the foreground object. It's notable that in the first case, when inserting the cruise, it is actually the view from the back of the reference image.

C.6. Comparison with Anydoor

Table 9 reports quantitative results on SAM-FB and Rank from Human Evaluation (RfHE) on in-the-wild im-

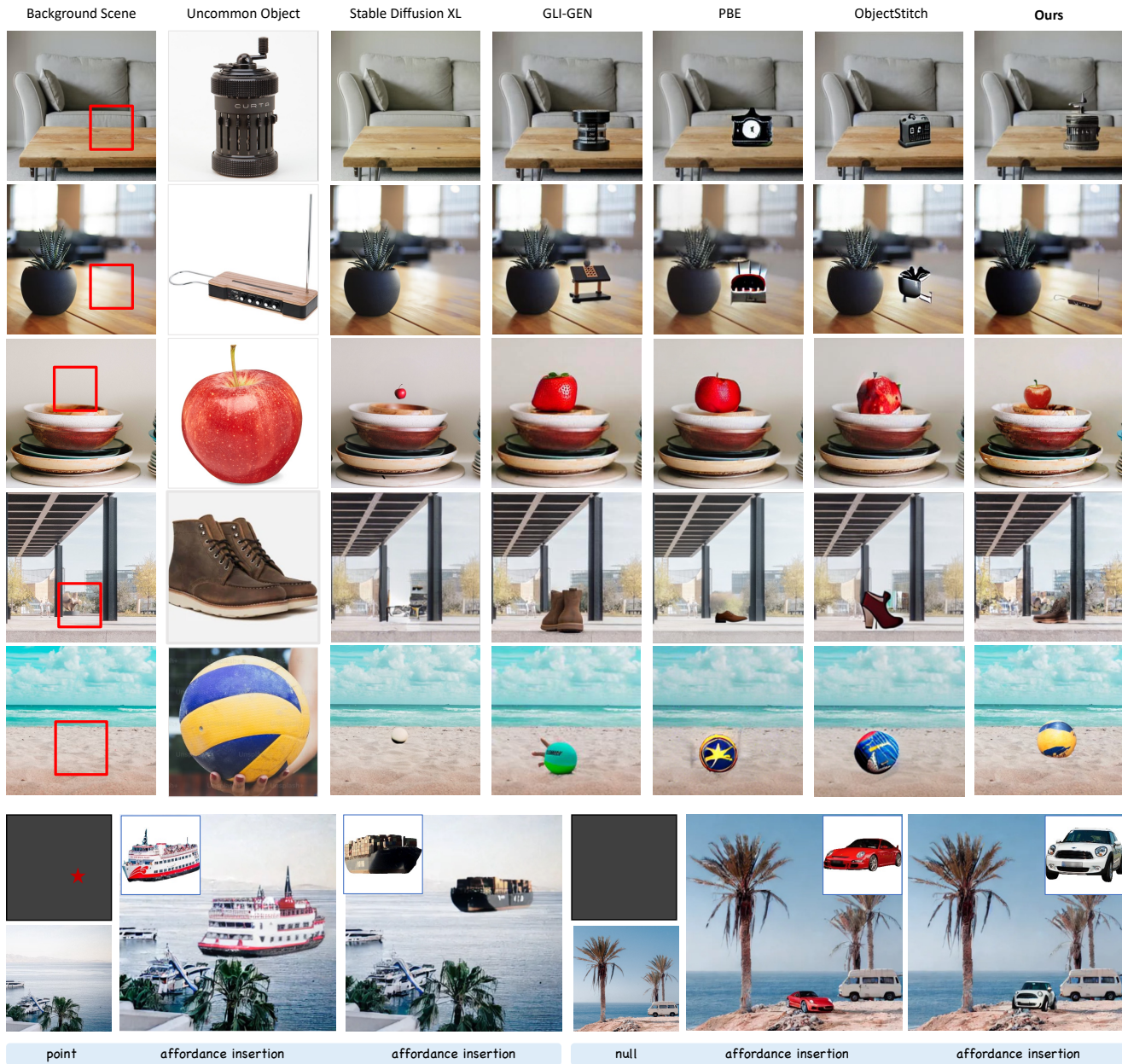


Figure 15. Example of in-the-wild insertion results with details. Our model could keep the appearance better and adjust the foreground’s properties better compared with SD [42], GLI-GEN [30] and PBE [49] on common objects. In the last row, the model generated reasonable insertion when provided ambiguous prompts.

Method	Anydoor	Ours
CLIP Score (↑)	0.8209	0.8658
DINO Score (↑)	0.667	0.693
RfHE(↓)	<u>2.18</u>	<u>2.21</u>

Table 9. Anydoor comparison

ages from web (*Unsplash*). Users prefer MADD for more reasonable insertion (Figure 16). Anydoor introduces arti-

facts around objects.

C.7. Video Demo

Please refer to the video demo in the attachment.

C.8. Failure Cases

Figure 17 shows some failure cases when using the model to perform affordance insertion. Generally, when prompted null position, it requires the model to search for a

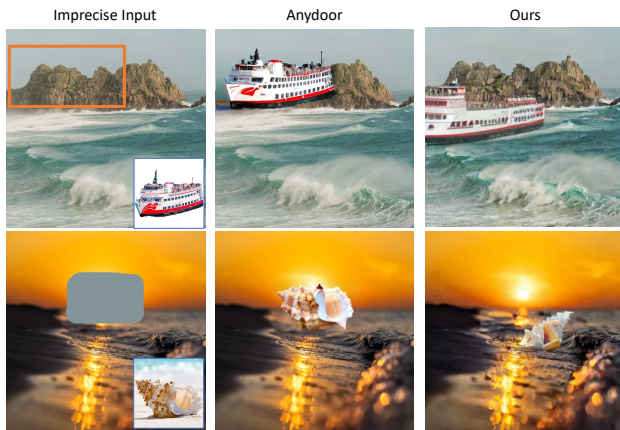


Figure 16. Affordance insertion compare with Anydoor



Figure 17. Some failure cases when using our model to perform affordance insertion.

possible position to insert the object. However, if there are already similar objects in the scene *e.g.*, traffic light in the first row, it is easy to mislead the model and end up with inserting nothing. When the background is too complex and the foreground object is too small, such as a vegetable in a supermarket shown in the second row, it is also difficult for the model to insert the object correctly.